tates formed during tempering. The cavities tended to facet strongly onto the low index planes due to their lower surface energy. The maximum cavity swelling (6.6% and 5.2%) occurred in Chinese RAFM and T91 steels irradiated at room temperature. Moreover, typical bimodal cavity size distributions were observed in both Chinese RAFM and T91 steels irradiated with Kr ions at 450 ℃. Base on the microstructural evolution of two different irradiated matensitic steels at the same condition, it reveals that T91 steel have a better irradiation swelling-resistance than Chinese RAFM steel.

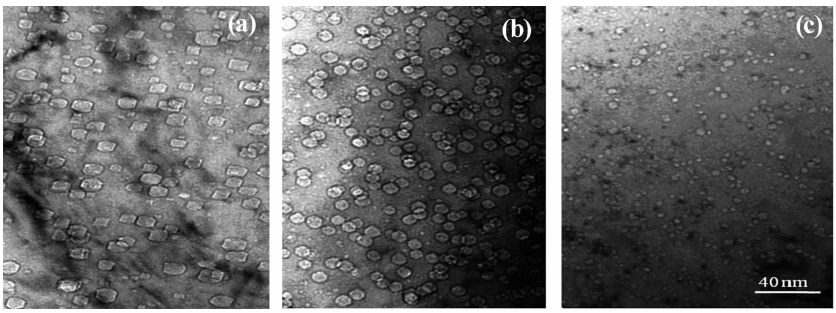

Fig. 2 Microstructure of cavities in Japan T91 steel at different irradiation conditions. (a) 31 dpa, RT; (b) 28 dpa, 450 ℃; (c) 31 dpa, 550 ℃.

3 - 7 Mechanical Properties and Microstructure of 316LN Weld Metal

Li Bingsheng, Dai Yong[1] and Wang Zhiguang

Fig. 1(a) shows the electron beam (EB) welded 316LN plate taken from a mini-tensile sample. The width of the weld zone and heat affected zone (HAZ) is 1 and 0.5 mm respectively. The grain morphology is totally different from the base metal. Fig. 1(b) shows the mean gain size for the base metal is about 55 μm.

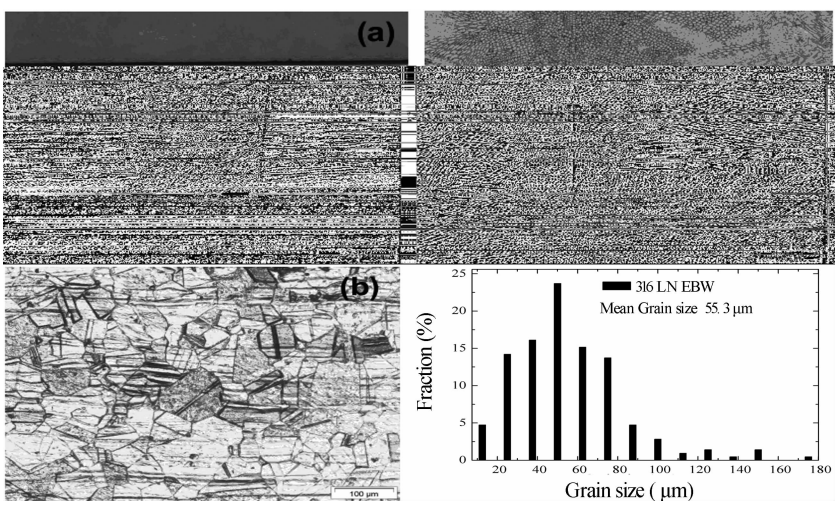

Fig. 1 Metallography morphology of weld zone (a) and base metal (b) and distribution of grain size.

The micro-hardness data were measured perpendicular to the weld center along the line from base metal, HAZ and weld zone, as shown in Fig. 2(a). The hardness value of 316LN base metal is around 170 HV measured with a test weight of 0.2 N. Hardening in the weld metal and the adjacent HAZ is more

1 Laboratory of Nuclear Material, Paul Scherrer Institut.

clearly observed and gives a value about 185 HV. Welding heat affects the weld joint both in hardening and softening. After tensile tests, significant deformation hardening was found by the micro-hardness test. In the weld zone, the hardness increases about a factor of 1.6, as shown in Fig. 2(b).

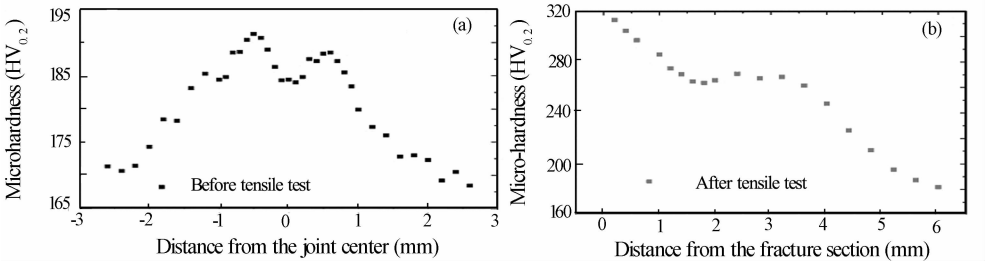

Fig. 2 Micro-hardness of the base and the weld metal before (a) and after the tensile test (b).

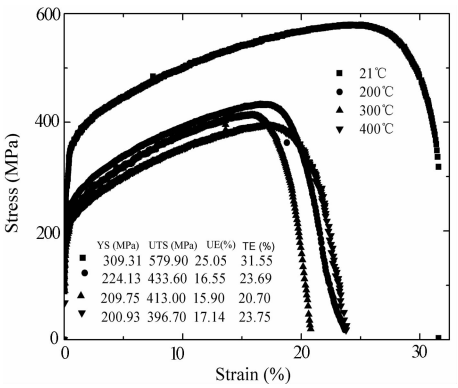

Fig. 3 Tensile stress-strain curves of 316 LN-EBW samples.

The tensile test was performed in hotlab. The same nominal strain rate, 1×10^{-3}/s, was used for all the tests. The test results are given in Fig. 3. With increasing test temperatures from room temperature to 400 ℃, the yield stress (YS) and ultimate tensile strength (UTS) decreases while the uniform elongation (UE) and total elongation (TE) firstly decreases, and then increases.

Dimple structures were observed by using scanning electron microscopy (SEM) on the fracture surface, indicating the ductile failure. Metallography analysis shows the fracture location at the center of weld zone, as shown in Fig. 4.

Some deformed zones were observed by transmission electron microscopy (TEM). Complex of stack fault and tangle dislocations in the deformed sample which was deformed 10% and the tensile test was at RT, as shown in Fig. 5(a). Increasing deformation to 25%, twins were formed (Fig. 5(b)), as the same for the sample which was deformed 20% at 200 ℃ (Fig. 5(c)). However, only tangle dislocations in the sample which was deformed 10% at 300 ℃, as shown in Fig. 5(d).

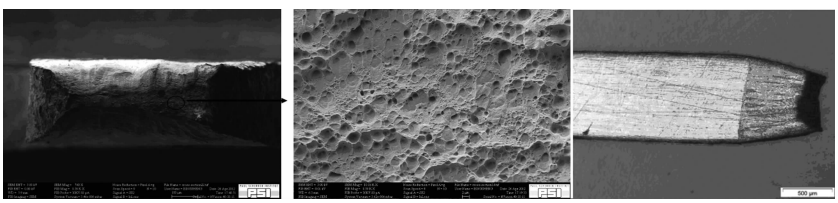

Fig. 4 The morphology of fracture surface tested by SEM and location tested by using optical microscopy.

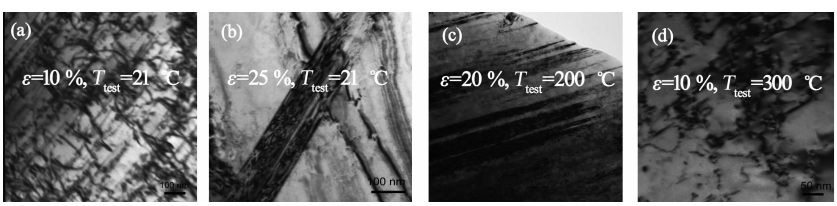

Fig. 5 Microstructure of deformed samples; (a) tested at RT with strain 10%; (b) tested at RT with 25% strain; (c) tested at 200 ℃ with 20% strain and (d) tested at 300 ℃ with 10% strain.